International Journal of Offshore and Polar Engineering (ISSN 1053-5381)
http://www.isope.org/publications/publications.htm

Vol. 27, No. 4, December 2017, pp. 423–432; https://doi.org/10.17736/ijope.2017.mmr18

Hull Form Multi-Objective Optimization for a Container Ship with Neumann–Michell Theory and Approximation Model

Xiaoyi Liu, Min Zhao* and Decheng Wan*
State Key Laboratory of Ocean Engineering, School of Naval Architecture, Ocean and Civil Engineering
Shanghai Jiao Tong University, Shanghai, China

Jianwei Wu
Wuhan Secondary Ship Design and Research Institute
Wuhan, China

With the continuous development of the shipbuilding industry and shipping business, hydrodynamic optimization of hull forms has drawn the attention of both academia and industry. This paper reports the details of an efficient, numerical, design optimization tool for hull form for container ships. This tool is composed of three functional modules: hull form deformation, hydrodynamic performance prediction, and optimization. The free-form deformation (FFD) and radial basis function (RBF) methods are employed to modify the ship hull globally and locally, respectively. To reduce the cost of the numerical optimization, which is always a challenging problem, a new potential theory, the Neumann–Michell (NM) theory, and the approximation model are adopted. In addition, the analysis of variance (ANOVA) method is used to represent the influence of each design variable on the objective functions. The high efficiency is illustrated by the optimization for a container ship. Wave resistance coefficients at three design speeds are minimized, and a Pareto front of solutions is obtained. The optimal hulls are verified and analyzed by the NM theory and a Reynolds-averaged Navier–Stokes (RANS)-based computational fluid dynamics (CFD) solver. Numerical results confirm the availability and reliability of the optimization tool described.

INTRODUCTION

In recent decades, with the continuous development of the shipbuilding industry and various shipping businesses, hydrodynamic optimization of hull forms has drawn the attention of both academia and industry. The economic efficiency of container ships, in particular, depends mainly on hydrodynamic performance. To obtain a hull form with the best hydrodynamic performance, design engineers have devised some approaches with different hydrodynamic analysis methods, geometrical modification techniques, and optimization algorithms. However, because of the complexity of ship hydrodynamics and the great number of evaluations of objective functions in optimization, ship hull optimization is quite time consuming. To solve this problem, a combination of a new, efficient hydrodynamic analysis method and an approximation model is adopted as a feasible scheme for ship hull optimization.

Prediction of hydrodynamic performance for a ship is always a challenging part of the optimization process. The hydrodynamic analysis method should be not only efficient for a variety of hull forms to be evaluated, but also robust, which means that the distinction among hulls with slight modification can be recognized. In recent years, potential flow theory has been employed for hydrodynamic analysis. Suzuki et al. (2005) used a potential flow solver to evaluate the energy of secondary flow for a tanker hull form optimization based on the Hess–Smith (Hess and Smith, 1967) and Rankine source methods (Dawson, 1977). Baoji (2012) obtained an optimized hull form with minimum wave-making using the Rankine source and optimization methods. Recently, a new, efficient potential theory, designated the Neumann–Michell (NM) theory (Noblesse et al., 2013), has been integrated in the optimization process to evaluate the objective functions. The computation of the steady flow around a moving ship based on the NM theory is efficient and robust because of the theory's succinctness. Kim (2009) adopted a similar potential theory for optimizing a ship hull form.

Geometric modification is also an important module in the ship hull optimization process. An appropriate and effective technique has been sought by several researchers, who tested methods based on different theories. Kim (2009) modified the Wigley hull form based on parametric hull representation and the nonuniform rational b-spline (NURBS) surface, Peri et al. (2001) utilized Bézier patches to complete the modification of hull geometry, and Tahara et al. (2014) employed the free-form deformation (FFD) method to modify the shape of a Delft catamaran. For the sake of conciseness and flexibility, two ideal approaches including the radial basis function (RBF) and FFD methods are utilized in the present study. The FFD method is introduced to modify the ship hull globally, and the RBF method is adopted to modify the bulbous bow. Both methods are proven to be flexible and reasonable.

During a reliable global multi-objective optimization process, a number of individuals should be evaluated by several objective functions. Since the major drawback with the repeating process is the large computational costs, an efficient way to overcome this issue is to establish an approximation model instead of a complete numerical process for each design during the optimization process. Additionally, the approximation model is created based on some sample data, the design spaces of which are generated by the design of experiments (DOE) method, while the objective functions are evaluated by numerical tools. Based on a comparison of different methods, Simpson et al. (2004) pointed out that the

*ISOPE Member.
Received September 29, 2016; revised manuscript received by the editors March 30, 2017. The original version was submitted directly to the Journal.
KEY WORDS: OPTShip-SJTU, multi-objective optimization, Neumann–Michell theory, wave resistance, approximation model.

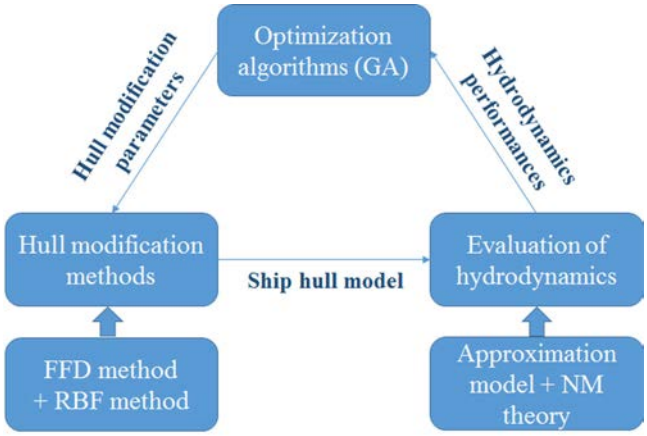

Fig. 1 Flowchart of in-house hydrodynamic optimization tool

most commonly used approximation method is the response surface method (RSM), which typically employs second-order polynomial models using least-squares regression techniques. Kriging is argued to be a more suitable method of constructing an approximation model. It is also called the design and analysis of computer experiment (DACE) model due to its advantages in computer experiments. The kriging method has many applications in structural and aerodynamic design but has seldom been used in hydrodynamic design. In this work, a kriging model is chosen to construct simplified approximations because of its flexibility and accuracy. Furthermore, a modified Latin hypercube design method called the optimized Latin hypercube sampling (OLHS) method is applied here to generate a DOE design matrix that satisfies the requirements of orthogonality and uniformity.

An algorithm is also a considerable influencing factor in the time cost of an optimization process and sometimes determines the "quality" of optimized solutions. Various algorithms have been investigated and compared to each other (Tahara et al., 2001; Pinto et al., 2007; Kim et al., 2011). Although the local optimization schemes are time saving, they are easily trapped in the local optimum when solving hull form design problems. To deal with the uncertainty of the sea environment and a container ship advancing at various speeds, a multi-objective optimization scheme should be adopted: then the optimal ship hulls will have consistent drag reduction over a large range of speeds compared to the original one. Therefore, a multi-objective genetic algorithm [a nondominated sorting genetic algorithm (NSGA-II)] has been employed to obtain a Pareto front.

In this paper, the hull form of a container ship is optimized for objective functions of wave resistance at three design speeds based on the in-house hydrodynamic optimization tool OPTShip-SJTU (Liu et al., 2016). Figure 1 is a flowchart of the optimization tool. The outline of the paper is as follows: In the next section, we introduce the NM theory, which is used for the hydrodynamic analysis. Then we demonstrate the geometric modification techniques, including the FFD and RBF methods. Next, we present the approximation model method used in this study, which is a combination of a kriging model and the optimized Latin hypercube sampling (OLHS) method. In the penultimate section, the algorithm NSGA-II, initialization, and results of the optimization process are introduced. Finally, four cases among Pareto-optimal solutions are selected for verification and analysis by a Reynolds-averaged Navier—Stokes (RANS)-based computational fluid dynamics (CFD) solver, naoe-FOAM-SJTU, which was developed based on OpenFOAM and has been validated in previous work (Shen and Wan, 2013; Liu and Wan, 2015).

Fr	0.17	0.21	0.25
C_w	0.561	0.711	0.942

Table 1 Wave resistance coefficients ($\times 10^{-3}$) predicted by the NM theory

WAVE RESISTANCE PREDICTED BY NM THEORY

The NM theory, proposed by Noblesse et al. (2013), is efficient and accurate for predicting wave resistance. It is an important attribute for a practical hydrodynamic analysis module in the hull form optimization process. In this study, the NM theory is employed to evaluate the drag of a ship hull. This theory can yield realistic predictions of wave drags at low computational cost. Owing to the simplicity and fast computation, the potential theory has been used for hull form optimization (Liu et al., 2016).

Introduction of NM Theory

When a ship steadily advances at a constant speed along a straight path in calm water of effectively infinite depth and lateral extent, the wave drag related to the waves generated by the advancing ship hull is of considerable practical importance because drag is a critical and dominant hydrodynamic factor in ship design. The NM theory is an efficient potential flow theory used to predict the ship waves. This theory is the modification of the Neumann–Kelvin (NK) theory based on a consistent linear flow model. The main difference between the two theories is that the line integral around the ship waterline that occurs in the classical NK boundary-integral flow representation is eliminated in the NM theory, so the NM theory expresses the flow about a steadily advancing ship hull in terms of a surface integral over the ship hull surface. Details of the NM theory are provided by Noblesse et al. (2013). The validation of this theory with different ship models is provided by Huang et al. (2013).

Application in a Container Ship

In this application, the NM theory is employed to predict the wave resistance of a typical container ship, the optimization of which will be detailed in a subsequent section. A mesh of 14,000 triangles is drawn as shown in Fig. 2. It takes approximately 90 s to predict the wave resistance at a specified speed by a PC with an Intel Core i7-4790k processor and 8 Gb of memory, although most of the PC's resources are idle. The wave resistance coefficients (C_w) in each Froude number (Fr) are listed in Table 1, which is one of the initializations of the entire optimization procedure.

The comparison of the simulation results obtained by the NM theory and by the RANS solver is presented in Table 2, which

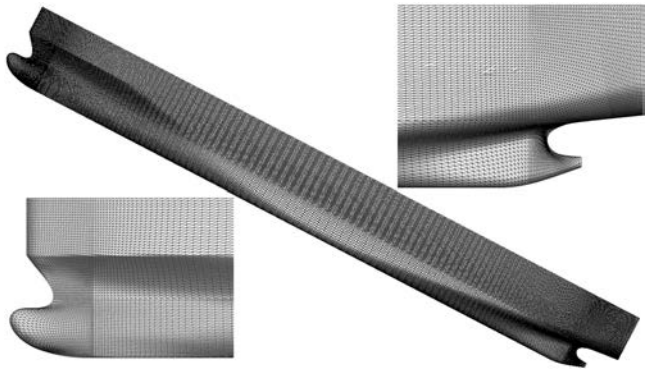

Fig. 2 Mesh of the container ship used by the NM theory

	NM			RANS	
Fr	C_w	C_f	C_t	C_t	Error
0.17	0.561	3.125	3.685	3.899	−5.80%
0.21	0.711	3.005	3.715	3.927	−5.69%
0.25	0.942	2.922	0.942	3.989	−3.22%

Table 2 Comparison of resistance coefficients ($\times 10^{-3}$) predicted by the NM theory and RANS solver

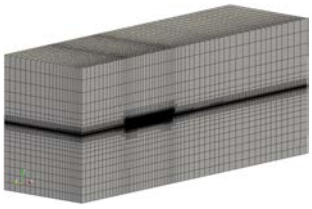

(a) Mesh computational domain

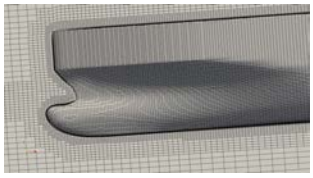

(b) Mesh of bow

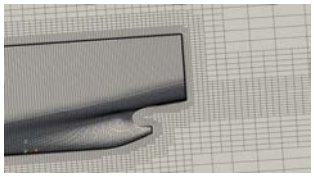

(c) Mesh of stern

Fig. 3 Mesh of container ship used by RANS solver

shows that the prediction of resistance coefficients by the NM theory is reliable. C_t and C_f represent the total resistance coefficient and friction resistance coefficient, respectively. Since the RANS solver only predicts total resistance in this study, the total resistance is used to compare the results obtained using the NM theory and the RANS solver. The error precision between the NM theory and the RANS solver is approximately 5%. Moreover, the NM theory requires only a few minutes using a PC to obtain the prediction, while the RANS solver requires several hours or even days, so the efficiency of the NM theory is higher than that of the RANS solver, which is much more critical to optimization at its early stage. Therefore, this practical prediction method based on the NM theory is quite suitable for the optimization work.

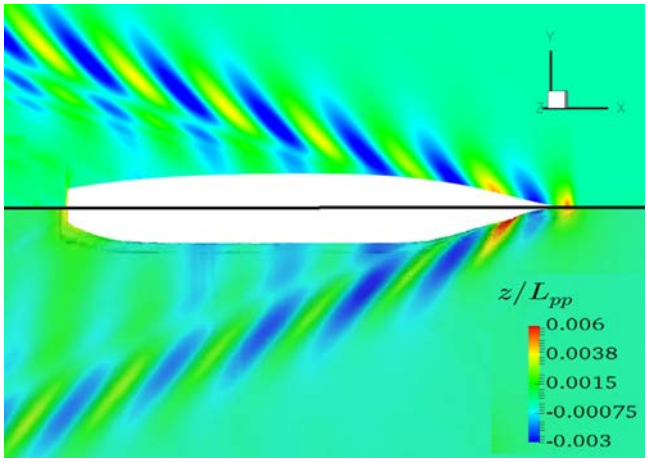

Fig. 4 Comparison of free surface predicted by RANS solver and the NM theory (top, NM theory; bottom, RANS solver)

The mesh used for the RANS solver is shown in Fig. 3. The domain contains 1.47 M mesh, which is refined around the bow and stern of the container ship and the free surface.

Figure 4 shows the comparison of the free surface around the ship predicted by the two methods. The free surface and wave resistance predicted by the NM theory are both reasonable.

SHIP HULL MODIFICATION METHODOLOGY

It is always an essential issue to find a method to modify the hull forms efficiently and rationally with low computational costs. In this study, two approaches are employed to deform the ship hull both locally and globally. The first is based on trivariate Bernstein polynomials (Sederberg and Parry, 1986) and the other is derived from an interpolation technique using an RBF (De Boer et al., 2007).

An FFD technique (Sederberg and Parry, 1986) is utilized to perform the deformation of solid geometric models in a free-form manner. The objects are embedded into a plastic parallelepiped and deformed along with it. The modification of the hull form is defined and controlled by use of the nodes that are used as design variables by the optimizer. Therefore, this method can be used to modify the global and local hulls. This method was also adopted in Tahara et al. (2008) and Campana et al. (2006), and more details about the scheme can be found in Sederberg and Parry (1986). In the present study, the FFD technique is utilized as a global modification tool for the ship's profile. The surface near the ship's bow is embedded into a parallelepiped on which the control points are imposed.

An RBF is a scalar function that is symmetric along the radial direction. De Boer et al. (2007) first applied it to a dynamic mesh method. In this study, the local modification of ship hull form is accomplished by using an RBF method. More details about the scheme can be found in De Boer et al. (2007).

In ship hull modification, the nodes on the ship hull surface consist of the fixed control nodes, movable control nodes, and free nodes:

(a) The fixed control nodes used to keep the hull surface near them unchanged are always on characteristic lines, such as the designed waterline, longitudinal line, and midship line.

(b) The movable control nodes used as design variables in the optimization procedure are always in special positions that deserve the attention of the designers.

(c) The free nodes are the nodes moving with the movable control nodes.

APPROXIMATION MODEL IN OPTIMIZATION

An approximation model is an important way to reduce the computational cost for optimization based on numerical methods. However, the approximation model becomes more complicated with the increase of design parameters and constraints, and the computational cost of surrogate construction and numerical simulation becomes unaffordable.

The DOE method is the best way to solve this problem, since it can reduce the number of simulation iterations and obtain a highly accurate approximation model. The most fundamental of the DOE methods is factorial design (Alvarez, 2000). A full factorial design contains all combinations of design parameters in every level. The number of required simulation times grows exponentially with the increase of the numbers of design parameters and levels. To avoid the increasing computational cost, various DOE methods have been proposed.

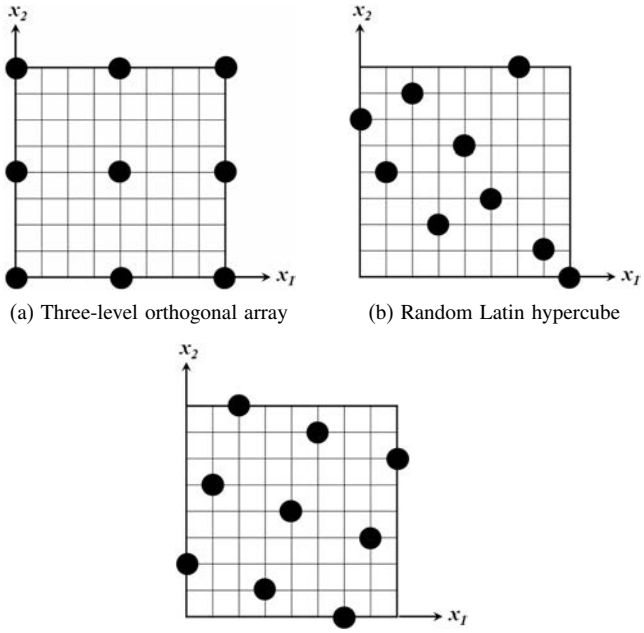

(a) Three-level orthogonal array (b) Random Latin hypercube

(c) Optimal Latin hypercube

Fig. 5 Three types of experimental design method

Optimal Latin hypercube design (Jin et al., 2005) is a modified Latin hypercube design in which the combination of factor levels for each factor is optimized, rather than being randomly and uniformly divided (the same number of divisions for all factors). The optimal Latin hypercube design is illustrated in Fig. 5 for a configuration with two factors and nine design points. Figure 5a shows the standard orthogonal array and Fig. 5b shows the random Latin hypercube design. The optimal Latin hypercube is shown in Fig. 5c, which covers nine levels of each design parameter. The design points of an optimal Latin hypercube are spread evenly within the design space. In this paper, optimal Latin hypercube design is used to generate the sample points of the approximation model.

A kriging model (Simpson et al., 1998) is developed using the best linear unbiased prediction method, which has its origins in mining and geostatistical applications. A kriging model combines a global model and local components:

$$y(x) = f(x) + z(x) \tag{1}$$

where $f(x)$ is the global model similar to a polynomial response surface model, and $z(x)$ is the local component used to measure the deviations from the global model.

The covariance matrix of $z(x)$ is given by

$$\mathrm{Cov}[z(x^{(i)}), z(x^{(j)})] = \sigma^2 R[R(x^{(i)}, x^{(j)})] \tag{2}$$

where R is the correlation matrix and $R(x^{(i)}, x^{(j)})$ is the correlation function between any two of the sample data points. In this work, a Gaussian correlation function of the following form is employed:

$$R(x^{(i)}, x^{(j)}) = \exp\left[-\sum_{k=1}^{n_v} \theta_k |x_k^{(i)} - x_k^{(j)}|^2\right] \tag{3}$$

where n_v is the number of design variables, θ_k are the unknown correlation parameters used to fit the model, and $x_k^{(i)}$ is the kth component of sample point $x^{(i)}$.

Using $f(x)$ and $z(x)$, the kriging model can build the surrogate model between the input and output variables. More details about the kriging model can be found in Simpson et al. (1998) and Liu et al. (2017).

OPTIMIZATION FORMULATION AND RESULTS

NSGA-II and Verification for a Test Function

The nondominated sorting genetic algorithms NSGA and NSGA-II (Srinivas and Deb, 1994; Deb et al., 2000) have been applied to various engineering optimization problems. Based on NSGA, NSGA-II employs a faster nondominated sorting approach and a selection operator that creates a mating pool by combining the parent and offspring populations and selecting the best N solutions (with respect to fitness and spread). Both test functions and engineering problems show that NSGA-II is able, for most problems, to find a much better spread of solutions and better convergence near the true Pareto-optimal front.

In this paper, the NSGA-II algorithm is adopted to drive the optimization procedure, which should be first verified for its effectiveness and logic. The verification objective function was first proposed by Deb et al. (2000):

$$\min \quad f_1(\mathbf{x}) = x_1, \tag{4}$$

$$\min \quad f_2(\mathbf{x}) = g * h, \tag{5}$$

$$\text{s.t.} \quad g = 1 + 10(n-1) + \sum_{i=2}^{n}(x_i^2 - 10\cos(4\pi x_i)), \tag{6}$$

$$h = 1 - \sqrt{\frac{f_1(x)}{g}}, \tag{7}$$

$$0 \le x_1 \le 1, -5 \le x_{2,\ldots,n} \le 5 \tag{8}$$

After 20,000 iterations of 100 generations and 200 individuals, the Pareto-optimal solutions are obtained as shown in Fig. 6. The Pareto front is plump and even enough to represent the optimal solutions. It shows that the optimization based on NSGA-II is reasonable and effective.

In this work, the NSGA-II algorithm is employed to obtain Pareto solutions in the ship hull optimization. The crossover rate is 0.75 and the mutation rate is 0.10. The number of generations is selected to be 1,000, with each generation containing 400 individuals.

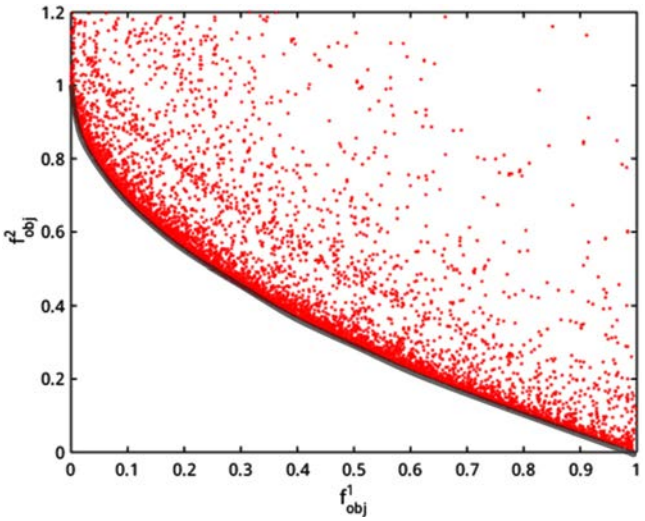

Fig. 6 Pareto front and individuals for test function generated by NSGA-II

Optimization Model of a Container Ship

The ship hull optimized in this paper is a Panamax container ship. The Froude numbers (Fr) of three design speeds for this container ship are 0.17, 0.21, and 0.25, and the optimization objective functions are chosen as the wave resistance at the three speeds. Some constraints should be considered to maintain the shape and characteristics of an optimal ship consistent with the original one. In this paper, principal parameters such as length and breadth are fixed, and the variations of displacement and wetted area are restrained in an acceptable range.

$$\min \quad f(\{x\}) = \{f^1_{\text{obj}}, f^2_{\text{obj}}, f^3_{\text{obj}}\}, \tag{9}$$

$$f^1_{\text{obj}} = C_{w,1}, \ \text{at} \ Fr = 0.17, \tag{10}$$

$$f^2_{\text{obj}} = C_{w,2}, \ \text{at} \ Fr = 0.21, \tag{11}$$

$$f^3_{\text{obj}} = C_{w,3}, \ \text{at} \ Fr = 0.25, \tag{12}$$

$$\{x\} = \{\Delta_1, \Delta_2, \Delta_3, x_1, x_2, y_1\}, \tag{13}$$

$$\text{s.t.} \quad g_1 = L^{\text{opt}}_{\text{pp}} - L^{\text{ori}}_{\text{pp}} = 0, \tag{14}$$

$$g_2 = T^{\text{opt}} - T^{\text{ori}} = 0, \tag{15}$$

$$g_3 = B^{\text{opt}} - B^{\text{ori}} = 0, \tag{16}$$

$$g_4 = \left| \frac{\nabla^{\text{opt}} - \nabla^{\text{ori}}}{\nabla^{\text{ori}}} \right| \le 1\%, \tag{17}$$

$$g_5 = \left| \frac{S^{\text{opt}}_{\text{wet}} - S^{\text{ori}}_{\text{wet}}}{S^{\text{ori}}_{\text{wet}}} \right| \le 1\% \tag{18}$$

where C_w is the wave resistance coefficient predicted by the NM theory varying with the changing hull forms, L_{pp} is the length between perpendiculars of the ship, T is the draft, B is the beam, ∇ is the displacement, and S_{wet} is the wetted area of the ship. According to the ITTC-1957 friction formula, the friction coefficient is determined by the Reynolds number. For the case of constant length of the ship and Reynolds number, the objective function of the wave resistance coefficient is equivalent to the total resistance coefficient.

The optimization variables are determined using the FFD and RBF methods. The FFD method is employed to modify the geometry of the ship hull globally. Three parallelepipeds shifting in different directions are illustrated in Fig. 7. For modifying the whole ship, a parallelepiped containing 150 control nodes is designed as shown in Fig. 7d. The green nodes can move only along the horizontal direction and are divided into two groups (on the left or right) that have the same value for distance in opposite directions, for the symmetry of the ship, while the red nodes are fixed. Figures 7b and 7c show two parallelepipeds containing fixed control nodes (red) and moving nodes (green) with longitudinal freedom. Three design variables x_1, x_2, y_1 represent the modification of these parallelepipeds. In terms of the local modification of the bulbous bow of the ship, three nodes with different moving directions are chosen for the RBF method. In Fig. 7a, nodes 1, 2, and 3 can only move longitudinally, horizontally, and vertically, respectively. Δ_1, Δ_2, and Δ_3 are the respective moving distances of the three nodes. The control nodes on the designed waterline, longitudinal line, and midship line are fixed. Some geometric constraints are imposed on the design variables, namely the displacement (∇), the wetted surface area (S_{wet}), and the principal dimensions of the ship. Detailed information regarding these constraints is summarized in Table 3.

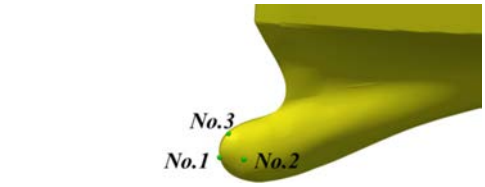

(a) Control nodes in RBF method

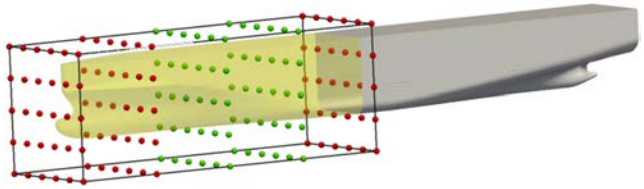

(b) Parallelepiped and control nodes moving longitudinally in fore-body

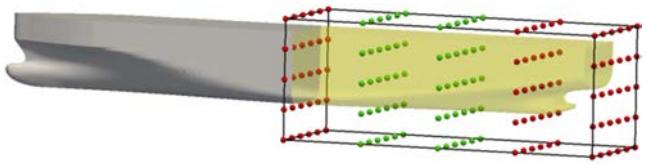

(c) Parallelepiped and control nodes moving longitudinally in aft-body

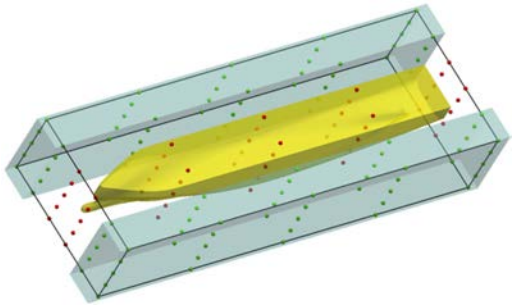

(d) Parallelepiped and control nodes moving horizontally

Fig. 7 Control node settings in RBF and FFD methods

Geometric constraints	Symbol	Value % Original
Length between perpendiculars	L_{pp}	0
Beam	B	0
Draft	T	0
Displacement	∇	1.0
Wetted area	S_{wet}	1.0
Variable constraints	Min. value	Max. value
V1(Δ_1/L_{pp})	−0.002	0.002
V2(Δ_2/L_{pp})	−0.002	0.002
V3(Δ_3/L_{pp})	−0.002	0.002
V4(x_1/L_{pp})	−0.01	0.01
V5(x_2/L_{pp})	−0.01	0.01
V6(y_1/L_{pp})	−0.005	0.005

Table 3 Design constraints

Approximation Model

Based on the optimal Latin hypercube design method mentioned above, a series of 100 sample points with six design variables of hull modification are listed in Table 4. The wave resistance coefficients are predicted by the NM theory.

The approximation model between input variables and output functions is constructed using a kriging model with the series of 100 samples. The time reduction obtained with the approximation

Design no.	V1	V2	V3	V4	V5	V6	f^1_{obj}	f^2_{obj}	f^3_{obj}
1	0.0001010	−0.0004242	0.0002525	0.0093939	0.0093939	0.0007576	0.00052683	0.00069015	0.00083618
2	−0.0014343	0.0005455	−0.0009596	0.0001010	−0.0023232	−0.0019697	0.00039238	0.00059557	0.00086371
3–99	...	...	...	...	...	...	...	...	...
100	0.0007879	0.0013939	0.0005354	0.0075758	0.0075758	−0.0010606	0.00060028	0.00076144	0.00090925

Table 4 Experimental design of ship hull

	Model 1	Model 2	Model 3
Max. absolute (error) ($\times 10^{-4}$)	0.731	0.879	0.847
Avg. absolute (error) ($\times 10^{-4}$)	0.245	0.332	0.308
Root MSE ($\times 10^{-4}$)	0.316	0.407	0.356

Table 5 Error analysis for kriging model

model is significant. For example, if the number of generations is set as 1,000 while the population size is 400, the simulation will number 400,000 iterations, and the optimization process with three objectives would take approximately 10,000 h (more than 1 year). However, the time cost of using the in-house hydrodynamic optimization tool described in this paper is only 2.5 h. The time reduction would be more significant if the number of objective functions were to increase.

Table 5 presents an error analysis of three kriging models of three objective functions with the sample points, which includes the maximum absolute error, the average absolute error, and the root-mean-square error (RMSE). It can be concluded that the kriging models are effective in approximating the objective functions in design space.

Analysis of Variance (ANOVA)

The ANOVA test is adopted here to investigate different characteristics and trade-offs of the different ship hull forms with respect to the objective functions. The results of the ANOVA tests are illustrated in Fig. 8. The design variables Δ_1, Δ_2, Δ_3, x_1, x_2, and y_1 are represented as V1–V6.

Among six design variables, V1 (Δ_1) has a continuous marked impact on the three objective functions. The length and volume of the bulbous bow influence wave resistances at each speed. In terms of other variables, the objective functions are affected in different ways. The case of the lowest speed, V6 (y_1), which determines the stoutness of the ship, has a significant effect (61%) on the wave resistance, while the percentage becomes much lower at the middle and high speeds. V3 (Δ_3), which determines the vertical location of the bulbous bow, plays an important role at the middle and high speeds.

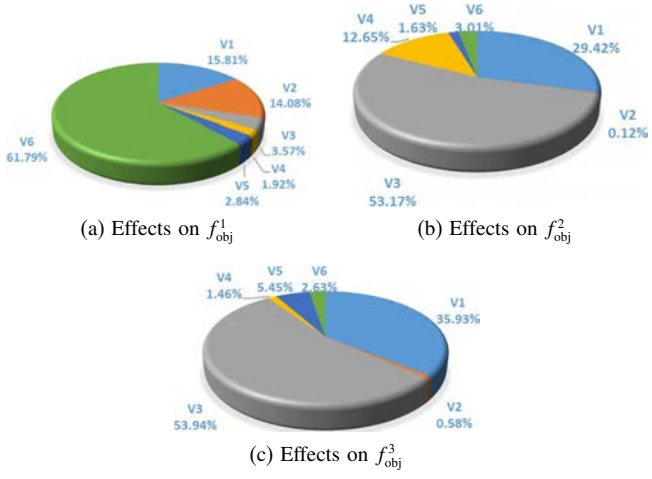

(a) Effects on f^1_{obj} (b) Effects on f^2_{obj}

(c) Effects on f^3_{obj}

Fig. 8 Results of ANOVA test

Optimization Results

The final nondominated and feasible designs from the optimization of the container ship are shown in Fig. 8, with the objectives being the wave resistance coefficients at three design speeds. Figures 9a–9c show the Pareto front in the two-dimensional views of each pair of objective functions, while Fig. 9d shows the full relationship of the Pareto front in a three-dimensional view. It is obvious that the Pareto-optimal solutions can be divided into two groups: the first is illustrated in the green box and the second in the yellow box in Fig. 9a. The first group seems like a plane with high f^3_{obj} as shown in Fig. 8d, and the "plane" degrades to a "line" on top of the Pareto front as shown in Figs. 8b and 8c. The Pareto-optimal solutions in the other group have larger f^1_{obj} and f^2_{obj}, but smaller f^3_{obj}. This phenomenon distinguishes the third objective function f^3_{obj} from the others, because it is inconsistent with either of them. It means that, if designers want a ship hull with better hydrodynamic performance at highest speeds, the wave resistance coefficients at lower speeds may be a little larger. On the other hand, a ship hull with good hydrodynamic performance at lower speeds can be obtained, but it may be not perfect at the highest speed.

The Pareto-optimal set provides over 9,000 solutions with drag reductions in different degrees at three given speeds. To verify these optimization results, three typical optimal hull forms, denoted cases 1–3, are chosen for further analysis, each having a minimum wave resistance coefficient for a given speed. Their design variables and body plans are illustrated in Figs. 10 and 11 and are summarized in Table 6.

Table 6 shows that the variables of V1–V5 have the same symbol for three optimal hulls. The optimal hulls have a longer, thinner, and lower-location bulbous bow. V2 and V3 (Δ_2, Δ_3) have smaller values in case 3 than in cases 1 and 2, which means that the bulbous bow at lower speeds needs to be much thinner and lower. However, the larger V1 (Δ_1) means that the container ship merits a longer bulbous bow at high speed. V4 and V5 (x_1, x_2), which mostly determine the location and shape of amidships, have a negative value in each case, which means that the amidships is moving to the rear, while the fore-body becomes longer and the aft-body becomes shorter. V6 has a positive value in case 2 and negative values in cases 1 and 3, which means that the ships with thinner hulls may exhibit better hydrodynamic performance at high and low speeds but not at middle speeds. In terms of the reduction of wave resistance coefficients, f^1_{obj} and f^2_{obj} have a larger reduction than f^3_{obj}. It is likely that the original hull is designed for high speed and not the lower speed.

Verification of Selected Designs and Approximation Model

The hydrodynamic performance of each case is predicted by two simulation tools, the NM theory and a RANS solver, to assess

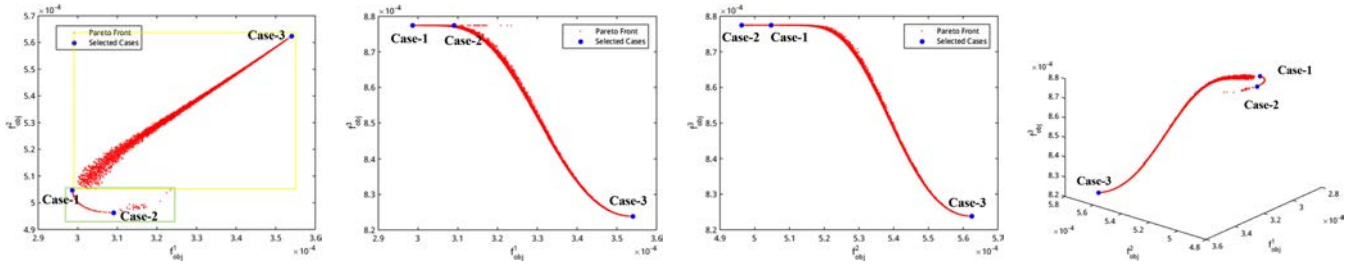

(a) Pareto front in f^1_{obj} and f^3_{obj} (b) Pareto front in f^1_{obj} and f^2_{obj} (c) Pareto front in f^2_{obj} and f^3_{obj} (d) Pareto front in f^1_{obj}, f^2_{obj} and f^3_{obj}

Fig. 9 Pareto front and selected cases in objective function space

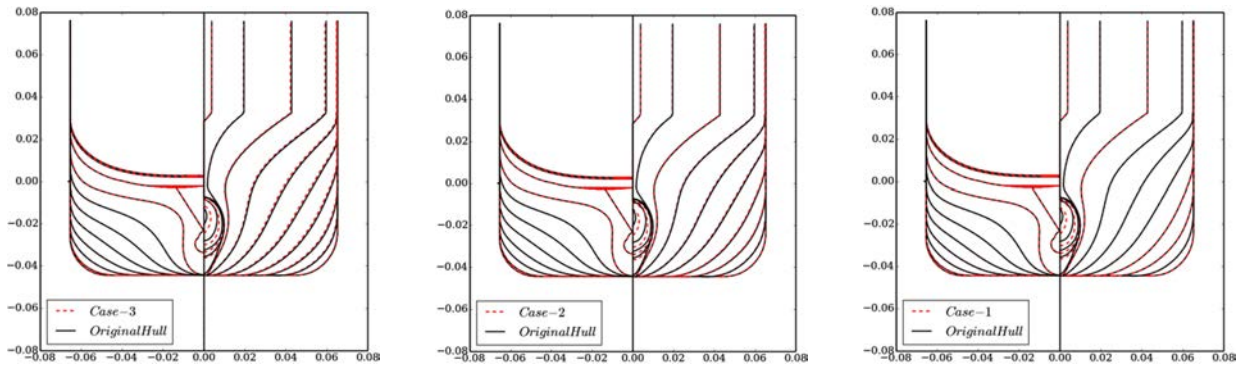

Fig. 10 Comparison of body plans for each selected case and original hull in transverse section

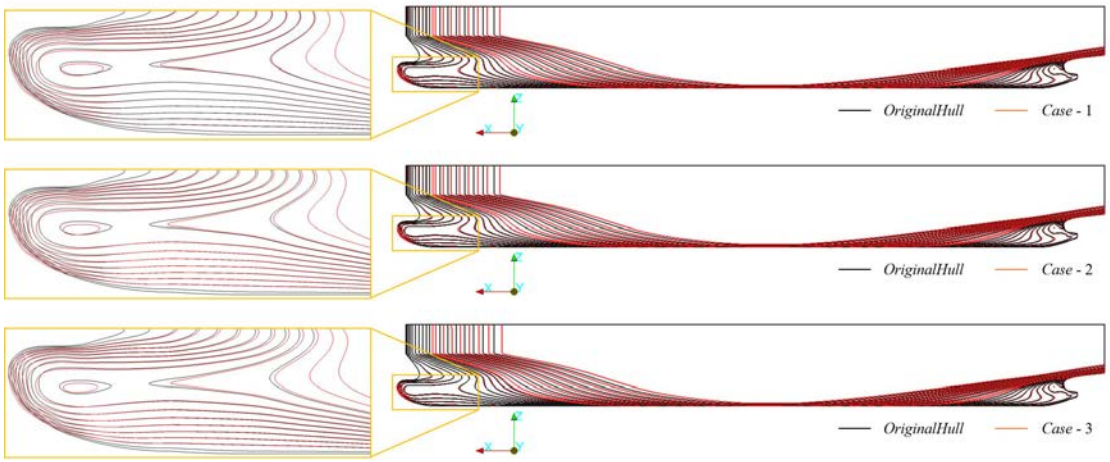

Fig. 11 Comparison of body plans for each selected case and original hull in longitudinal section

	Original	Case 1	Case 2	Case 3
Δ_1	0	0.00154	0.00152	0.00181
Δ_2	0	−0.00021	−0.00028	−0.00002
Δ_3	0	−0.00089	−0.00079	−0.00041
x_1	0	−0.00459	−0.00123	−0.00959
x_2	0	−0.00107	−0.00072	−0.00092
y_1	0	−0.00041	0.00033	−0.00075
Displacement % (original)	0	−0.14%	0.07%	−0.13%
Wetted area % (original)	0	−0.08%	0.03%	−0.10%
f^1_{obj} (%) (original)	0.000561	0.000298 (46.7%)	0.000309 (44.9%)	0.000354 (36.8%)
f^2_{obj} (%) (original)	0.000711	0.000504 (28.9%)	0.000496 (30.2%)	0.000563 (20.8%)
f^3_{obj} (%) (original)	0.000942	0.000878 (6.87%)	0.000878 (6.87%)	0.000824 (12.6%)

Table 6 Comparison of design variables and performance between original ship hull and three selected cases

Fr		0.17			0.21			0.25		
Components		C_w	C_f	C_t	C_w	C_f	C_t	C_w	C_f	C_t
Original	NM	0.561	3.125	3.685	0.711	3.005	3.715	0.942	2.922	3.864
	RANS	/	/	3.899	/	/	3.927	/	/	3.989
Case 1	NM	0.309	3.125	3.434	0.526	3.005	3.531	0.877	2.922	3.799
	RANS	/	/	3.796	/	/	3.879	/	/	3.899
Case 2	NM	0.332	3.125	3.457	0.505	3.005	3.51	0.887	2.922	3.809
	RANS	/	/	3.804	/	/	3.841	/	/	3.913
Case 3	NM	0.373	3.125	3.498	0.561	3.005	3.566	0.812	2.922	3.734
	RANS	/	/	3.864	/	/	3.877	/	/	3.875

Table 7 Comparison of the optimization results ($\times 10^{-3}$) obtained using the NM theory and a RANS solver

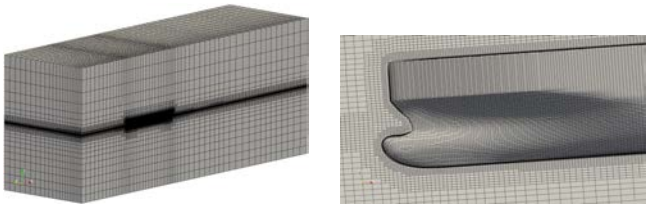

(a) (b)

Fig. 12 Comparison of total resistance coefficients predicted by (a) the NM theory and (b) a RANS solver

the validity of the optimization results based on the approximation technique. The comparison of the optimization results obtained using the NM and RANS methods are presented in Table 7 and Fig. 12. C_f and C_t represent the coefficients of friction resistance and total resistance, respectively.

The results predicted by the NM theory are in agreement with those calculated using the approximation model, which proves the validity of the approximation model constructed by 100 sample cases. However, there are still some errors between them, which means that additional attempts and more advanced approximation methods are needed. We observe that the results predicted using the NM theory have more differences from those predicted using a RANS solver, especially at lower speeds, while the total resistance coefficients are closer at high speed.

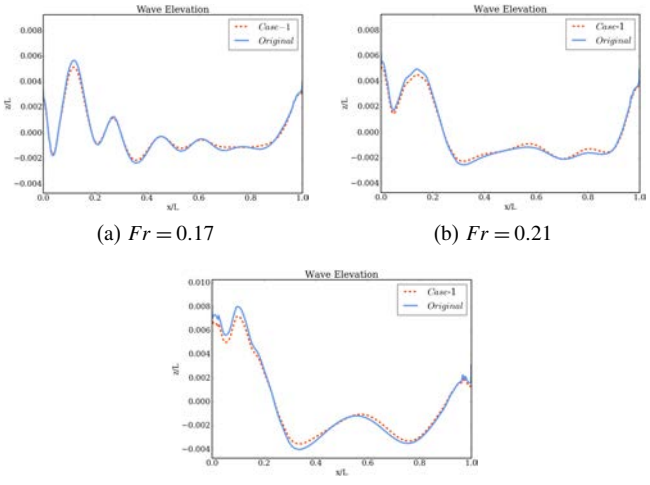

(a) $Fr = 0.17$ (b) $Fr = 0.21$

(c) $Fr = 0.21$

Fig. 13 Comparison of the wave elevations between original hull and case 1 at three speeds

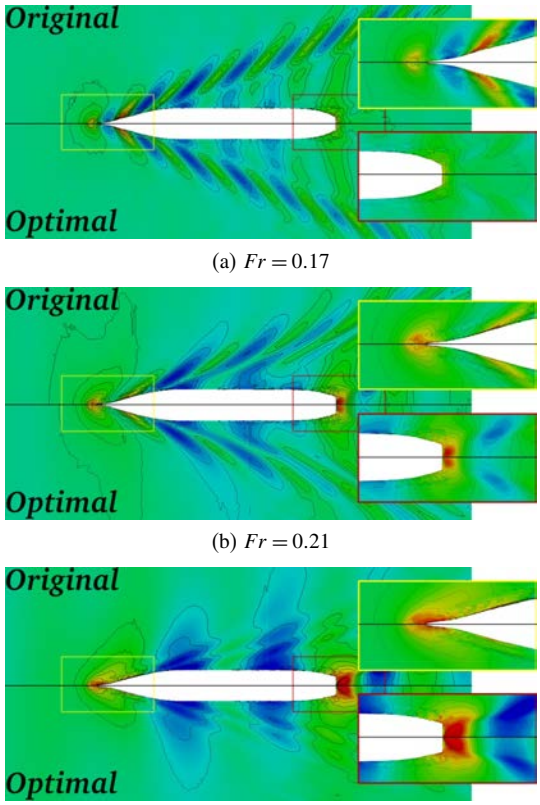

(a) $Fr = 0.17$

(b) $Fr = 0.21$

(c) $Fr = 0.25$

Fig. 14 Comparison of the free surface predicted by a RANS solver between the original hull and hull case 1 at three speeds

The wave elevation comparison is illustrated in Fig. 13. From the perspective of waves generated by the ship hull, case 1 has a lower wave amplitude than the original hull at all three speeds. The first wave crest generated by the ship hull is always lower, which is mainly due to the fact that the bulbous bow becomes longer and thinner and performs better in restraining the wave making. Thus, the pressure caused by wave making on the bow will be lower. The lower wave making and pressure on the bow make the optimal hull's wave resistance coefficient lower.

A high-fidelity RANS solver is employed here to predict the hydrodynamic performance and flow physics for selected hulls advancing at the design speeds. The simulation results of resistance coefficients are summarized in Table 7, and the free surface around hull case 1 is illustrated in Fig. 14. The comparison of total resistance coefficients between the original hull and selected optimal hulls presented in Table 7 shows the same trend as that

predicted by the NM theory, but the reduction of resistance coefficients is much less than that obtained using the approximation model and the NM theory. There are two possible reasons for this. First, the NM theory exhibits unrealistically large oscillations with respect to ship speeds, as do other analytical methods (Noblesse et al., 2013). Second, the total resistance coefficient calculated using the NM theory plus an ITTC friction formula disregards the coupling effect between friction and wave resistance. Nevertheless, each of the selected hulls has an obvious advantage for various speeds. It can be concluded that the NM theory can be used in ship optimization design with such hull forms. The comparison of the free surfaces between original and optimal hulls shows that the wave caused by optimal hulls has smaller amplitudes at each speed. This result contributes to the reduction of the wave resistance and of the total resistance.

CONCLUSIONS

In the work described in this paper, experimental designs obtained using the optimal Latin hypercube method, a kriging model combined with the NM theory, and a modification module with both global and local techniques were subjected to a new numerical multi-objective optimization tool.

The FFD and RBF methods were combined to modify the global and local forms of the ship. The introduction of an approximation model and a DOE technique was found to clearly accelerate the optimization procedure.

A Panamax container ship was adopted as the original hull form, and the objective functions were the wave resistance coefficients at three different speeds. The bulbous bow and the entire shape were modified using RBF and FFD methods. Analysis of variables followed the construction of an approximation model with 100 sample cases. According to the optimization, the Pareto front was successfully obtained after 400,000 iterations of the evaluation for objective functions. Three cases were selected from over 9,000 Pareto solutions, and each was verified using the NM theory and a RANS solver. The optimal results confirmed the validity of the combination of the approximation method and the NM theory for a container ship hull form optimization.

Further work will focus on the extension of the performance evaluation associated with seakeeping and maneuvering. In addition, the efficiency and accuracy of the approximation model need more attention in order to provide a better optimization tool that can be applied in more disciplines.

ACKNOWLEDGEMENTS

This work was supported by the National Natural Science Foundation of China (Grant Nos. 51109132, 51779139) and the Specialized Research Fund for the Doctoral Program of Higher Education of China (Grant No. 20110073120015). Critical comments from reviewers are also greatly appreciated.

REFERENCES

Alvarez, L (2000). *Design Optimization Based on Genetic Programming*, PhD Thesis, University of Bradford, Bradford, UK.

Campana, EF, et al. (2006). "Simulation Based Design of Fast Multihull Ships," In: *Proc 26th Symp Naval Hydrodyn*, Rome, Italy.

Dawson, CW (1977). "A Practical Computer Method for Solving Ship Wave Problems," *Proc 2nd Int Conf Numer Ship Hydrodyn*, Berkeley, CA, USA, 30–38.

De Boer, A, van der Schoot, MS, and Bijl, H (2007). "Mesh Deformation Based on Radial Basis Function Interpolation," *Comput Struct*, 85(11–14), 784–795. https://doi.org/10.1016/j.compstruc.2007.01.013.

Deb, K, Agrawal, S, Pratap, A, and Meyarivan, T (2000). "A Fast Elitist Non-Dominated Sorting Genetic Algorithm for Multi-Objective Optimization: NSGA-II," *Proc 6th Int Conf Parallel Problem Solving Nature*, Paris, France, 849–858.

Hess, JL, and Smith, AMO (1967). "Calculation of Potential Flow About Arbitrary Bodies," *Prog Aerosp Sci*, 8(8), 1–138. https://doi.org/10.1016/0376-0421(67)90003-6.

Huang, FX, Yang, C, and Noblesse, F (2013). "Numerical Implementation and Validation of the Neumann–Michell Theory of Ship Waves," *Eur J Mech B Fluid*, 42(6), 47–68. https://doi.org/10.1016/j.euromechflu.2013.05.002.

Jin, RC, Chen, W, and Sudjianto, A (2005). "An Efficient Algorithm for Constructing Optimal Design of Computer Experiments," *J Stat Plann Inference*, 134(1), 268–287. https://doi.org/10.1016/j.jspi.2004.02.014.

Kim, HY (2009). *Multi-Objective Optimization for Ship Hull Form Design*, PhD Thesis, George Mason University, Fairfax, VA, USA.

Kim, HY, Yang, C, Jeong, S, and Noblesse, F (2011). "Hull Form Design Exploration Based on Response Surface Method," *Proc 21st Int Offshore Polar Eng Conf*, Maui, HI, USA, ISOPE, 4, 816–825.

Liu, XY, and Wan, DC (2015). "Numerical Simulation of Ship Yaw Maneuvering in Deep and Shallow Water," *Proc 25th Int Ocean Polar Eng Conf*, Kona, HI, USA, ISOPE, 4, 1200–1206.

Liu, XY, Wu, JW, and Wan, DC (2016). "Multi-Objective Optimization for a Surface Combatant Using Neumann–Michell Theory and Approximation Model," Presented at *12th Int Conf Hydrodyn*, Egmond aan Zee, The Netherlands.

Liu, XY, Yuan, QQ, Zhao, M, Ge, T, and Cui, WC (2017). "Multiple Objective Multidisciplinary Design Optimization of Heavier-Than-Water Underwater Vehicle Using CFD and Approximation Model," *J Mar Sci Technol Jpn*, 22(1), 135–148. https://doi.org/10.1007/s00773-016-0399-5.

Noblesse, F, Huang, FX, and Yang, C (2013). "The Neumann-Michell Theory of Ship Waves," *J Eng Math*, 79(1), 51–71. https://doi.org/10.1007/s10665-012-9568-7.

Peri, D, Rossetti, M, and Campana, EF (2001). "Design Optimization of Ship Hulls via CFD Techniques," *J Ship Res*, 45(2), 140–149.

Pinto, A, Peri, D, and Campana, EF (2007). "Multiobjective Optimization of a Containership Using Deterministic Particle Swarm Optimization," *J Ship Res*, 51(3), 217–228.

Sederberg, TW, and Parry, SR (1986). "Free-Form Deformation of Solid Geometric Models," *ACM SIGGRAPH Comput Graphics*, 20(4), 151–160. https://doi.org/10.1145/15886.15903.

Shen, ZR, and Wan, DC (2013). "RANS Computations of Added Resistance and Motions of a Ship in Head Waves," *Int J Offshore Polar Eng*, ISOPE, 23(4), 264–271.

Simpson TW, Mauery TM, Korte JJ, and Mistree, F (1998). *Comparison of Response Surface and Kriging Models in the Multidisciplinary Design of an Aerospike Nozzle*, Technical Report NASA/CR-1998-206935, NASA Langley Research Center, Hampton, VA, USA.

Simpson, TW, et al. (2004). "Approximation Methods in Multidisciplinary Analysis and Optimization: A Panel Discussion," *Struct Multidiscip Optim*, 27(5), 302–313. https://doi.org/10.1007/s00158-004-0389-9.

Srinivas, N, and Deb, K (1994). "Multiobjective Optimization Using Nondominated Sorting in Genetic Algorithms," *Evol Comput*, 2(3), 221–248. https://doi.org/10.1162/evco.1994.2.3.221.

Suzuki, K, Kai, H, and Kashiwabara, S (2005). "Studies on the Optimization of Stern Hull Form Based on a Potential Flow Solver," *J Mar Sci Technol*, 10(2), 61–69. https://doi.org/10.1007/s00773-005-0198-x.

Tahara, Y, Paterson, EG, Stern, F, and Himeno, Y (2001). "Flow- and Wave-Field Optimization of Surface Combatants Using CFD-Based Optimization Methods," *Proc 23rd Symp Naval Hydrodyn*, Val De Reuil, France, 243–261.

Tahara, Y, Peri, D, Campana, EF, and Stern, F (2008). "Single and Multiobjective Design Optimization of a Fast Multihull Ship: Numerical and Experimental Results," *J Mar Sci Technol*, 16(4), 412–433. https://doi.org/10.1007/s00773-011-0137-y.

Tahara, Y, et al. (2014). "CFD-Based Multiobjective Stochastic Optimization of a Waterjet Propelled High Speed Ship," In: *Proc 29th Symp Naval Hydrodyn*, Gothenburg, Sweden.